Genet. Res., Camb. (1990), **56**, *pp.* 167–178 *With 4 text-figures Printed in Great Britain*

The hairy ears (*Eh*) mutation is closely associated with a chromosomal rearrangement in mouse chromosome 15

MURIEL T. DAVISSON*, THOMAS H. RODERICK, ELLEN C. AKESON, NORMAN L. HAWES AND HOPE O. SWEET
The Jackson Laboratory, Bar Harbor, ME 04609, USA

(*Received 29 March 1990 and in revised form 21 May 1990*)

Summary

The mouse mutation hairy ears (*Eh*) originated in a neutron irradiation experiment at Oak Ridge National Laboratory. Subsequent linkage studies with *Eh* and other loci on Chr 15 suggested that it is associated with a chromosomal rearrangement that inhibits recombination since it shows tight linkage with several loci occupying the region extending from congenital goiter (*cog*) distal to caracul (*Ca*). We report here (1) linkage experiments confirming this effect on recombination and (2) meiotic and mitotic cytological studies that confirm the presence of a chromosomal rearrangement. The data are consistent with the hypothesis of a paracentric inversion in the distal half of Chr 15. The effect of the inversion extends over a minimum of 30 cM, taking into account the genetic data and the cytologically determined chromosomal involvement extending to the region of the telomere.

1. Introduction

Many mutations causing changes in visible phenotype or in protein-encoding loci have been induced or have arisen in mutagenesis experiments. Mice carrying such mutations are not always examined for chromosomal aberrations, depending largely on the laboratory where the mutation was induced or whether the laboratory was also screening for chromosome aberrations. These induced mutations are described in the literature and are retained as useful mutations, but the information that they were induced may be forgotten over time. Mutations carrying undetected chromosome aberration can drastically alter recombination results in subsequent mapping studies.

The hairy ears (*Eh*) mutation was discovered at Oak Ridge National Laboratory among the progeny of a male mouse who had been neutron-irradiated (post spermatogonial stages) (Bangham, 1965). In heterozygotes the pinna is reduced and appears to have extra hair, including a tuft of hair on the inner surface. *Eh* is homozygous lethal before birth (Bangham, 1968). In the Mouse Mutant Resource at The Jackson Laboratory we were simultaneously searching for the chromosomal location of three new mutations when we discovered that all three mutations appeared to be tightly linked to the *Eh* locus on Chromosome (Chr) 15; yet subsequent mapping studies clearly showed that the three loci mapped to different regions of Chr 15. The first locus, dominant megacolon (*Dom*), is located 36 cM from the centromere (Lane & Lui, 1984); the second, grey tremor (*gt*), maps 19 cM from *Ca*, probably proximal because of the distal position of *Ca* on the chromosome (Sidman *et al.* 1985); the third was a remutation (Ca^{7J}) at the caracul locus which is 51 cM from the centromere (data for *gt* and Ca^{7J} with *Eh* in this paper) (see Fig. 3). Published reports also show that *Eh* has low or no recombination with the additional loci, congenital goiter at 25 cM from the centromere (Beamer *et al.* 1987), belted (*bt*) located between *Dom* and *Ca* (Russell & McFarland, 1977), and motor end-plate disease (*med*), velvet (*Ve*), and perinatal lethal (*ple*), all of which map to the same location as *Ca* (Guenet, 1976; Guenet, 1980; Beier *et al.* 1989, respectively).

We report here the results of genetic crosses and analyses of G-banded mitotic chromosomes and synaptonemal complexes from *Eh*/+ heterozygotes that provide evidence that the *Eh* mutation is associated with a chromosomal rearrangement in the distal end of Chr 15. To analyze the effect of *Eh* on recombination we have created a marker stock for Chr 15–STOCK *uw* $Gpt\text{-}1^{b}$ $Gdc\text{-}1^{a}$ bt^{2J} – which we will continue to maintain.

* Corresponding author.

2. Materials and methods

All mice used for these studies originated from the research and production colonies of The Jackson Laboratory. All linkage crosses were made in our colonies. The *Eh* mutation is maintained on the C57BL/6JEi(B6) genetic background in The Jackson Laboratory's Mouse Mutant Resource colony. The other mutant genes used are maintained in the Mouse Mutant Resource; the inversions are maintained in Dr Roderick's research colony.

(i) *Genetic crosses*

Preliminary backcrosses with and without *Eh* present used the Chr 15 isozyme markers glutamic pyruvic transaminase-1 (*Gpt-1*) and glycerol 3-phosphate dehydrogenase (*Gdc-1*) in one set of crosses and the visible markers underwhite (*uw*) and belted-2J (bt^{2J}) with *Gdc-1* in a second set of crosses. To measure the effect of *Eh* on recombination along the entire length of Chr 15 in one cross a linkage testing stock for Chr 15 was created. We crossed B6-*uw* $Gpt\text{-}1^a$ bt^{2J} $Gdc\text{-}1^b$ mice from a mutant strain homozygous for the visible markers *uw* and bt^{2J} to NZB/BlNJ $Gpt\text{-}1^b$ $Gdc\text{-}1^b$. An F2 mouse from this cross was mated to a mouse of the inbred *Mus musculus castaneus*, CASA/Rk $Gpt\text{-}1^b$ $Gdc\text{-}1^a$ strain. Subsequently, the stock was maintained by brother × sister matings, selecting first for breeders that carried recombinant chromosomes and then for *uw* bt^{2J}/*uw* bt^{2J} breeders homozygous for the $Gpt\text{-}1^b$ and $Gdc\text{-}1^a$ alleles.

The new Chr 15 marker stock is homozygous for *uw*, bt^{2J} and the rare alleles $Gpt\text{-}1^b$ and $Gdc\text{-}1^a$. Mice from this stock were crossed to B6-*Eh*/+ mice and F1s were backcrossed to the marker stock. Simultaneous control crosses were made by mating mice of the marker stock to B6 mice without *Eh*. Most of the linkage crosses were done simultaneously with construction of the marker stock, so not all loci were segregating in each cross. Crosses were also made with a stock homozygous for inversion In(15)18Rk, which comprises approximately the proximal half of Chr 15. Mice doubly heterozygous for *Eh* and In18Rk were outcrossed to B6 mice for linkage analysis.

(ii) *Anaphase bridge analysis*

To determine the frequency of anaphase bridges, one testis was removed, sectioned, stained, and examined with a light microscope. The frequency was determined by the number of first meiotic anaphases (AI) showing intact bridges divided by the total number of AI divisions scored. Approximately 20 AI cells per male were scored for anaphase bridges, which is usually sufficient to ascertain the presence of a paracentric inversion larger than 25 cM (Roderick, 1971).

(iii) *Isozyme scoring*

GPT-1 was scored using a modification of the method of Eicher & Womack (1977). The successful method we use is given in detail here because this is a difficult enzyme to assay. Tissue homogenates of 280 mg liver /0·5 ml distilled water plus 2 drops 10% Triton X-100 were held for 15 minutes at 4 °C. Supernatants were processed after centrifugation for 30 minutes at 27000 *g* and 4 °C. Samples were applied to Titan III cellulose acetate plates (Helena Laboratories), using 5 applications 0·5–1·0 cm from the cathodal end, and electrophoresed cathode to anode at 200 V for 45 minutes at room temperature. The buffer was 25 mM Trizma Base (T-1503) and 192 mM glycine (G-7126), pH 8·3. The staining mixture contained 600 mg D-L-alanine (A-7502), 30 mg α-ketoglutaric acid (K-1875), 3 drops 0·01 M KCN (Fisher Scientific Company, P-226), 9 drops TPN (N-0505) (10 mg/ml), 9 drops MTT (M-2128) (10 mg/ml), and 9 drops PMS (P-9625) (2·4 mg/ml) in 12 mls 0·2 M Tris-HCl, pH 8·0. Eighteen mls of 2% agar and 12 drops of undiluted L-glutamic dehydrogenase (G-2626) were added to the solution just prior to use. Drops were dispensed by Pasteur pipet. Plates were placed on a slide warmer at 37 °C and bands were read within 15 minutes. Heart homogenates were used when assaying retired breeders to avoid fatty supernatants.

GDC-1 mobility was scored using a modification of the protocol of Dr E. M. Eicher (personal communication). Liver supernatants were applied once 1·5 cm from the cathodal end of Titan III cellulose acetate plates and electrophoresed cathode to anode at 200 V for 45 minutes at room temperature using the same buffer as above at pH 8·5. The staining mixture contained 4 ml 0·2 M Tris-HCl pH 8·0, 0·25 ml DPN (N-7004) (66 mg/ml), 0·1 ml MTT, 0·1 ml PMS, and 0·5 ml DL-α-glycerophosphate (G-2138) 20 mg/ml. With agar overlay, the bands were read within minutes at room temperature. All chemicals except KCN were obtained from Sigma Chemical Company.

(iv) *Mitotic chromosome analysis*

Mitotic chromosome preparations were made from peripheral blood of female mice heterozygous for the *Eh* mutation following the method of Davisson & Akeson (1987). G-banded metaphase chromosomes were examined for any evidence of a chromosomal aberration. In addition, total length of the Chr 15 homologs was measured on photographs of G-banded chromosomes. Chromosomal measurements were made independently on coded karyotypes by two people who were not involved in the *Eh* study and did not know the purpose of the measurements.

(v) *Synaptonemal complex analysis*

To analyze synaptonemal complexes surface spread preparations of spermatocytes were made from two 4-week-old male mice doubly heterozygous for *Eh* and Rb(3.15)2Rk or Rb(5.15)4Lub (*Eh*+/+Rb) according to the method of Moses (Dresser & Moses, 1979; Moses, 1977). Both poly-lysine-coated and plastic film-coated slides were stained with 50% silver nitrate (Howell & Black, 1980). The stained poly-lysine-coated slides were examined by light microscopy and photographed using a Zeiss photomicroscope. The plastic coat of the plastic film-coated slides was floated off the slide onto a water surface and transferred to grids for electron microscopy and photographing.

(vi) *Meiotic analysis of metaphase I*

Air dried meiotic preparations were prepared according to the method of Evans *et al.* (1964). Metaphase I cells from 2 *Eh*/+ males were examined for the presence of abnormalities, especially translocation configurations.

Results

(i) *Linkage analysis*

Linkage data presented in Tables 1–5 (crosses 1–17) show clearly that *Eh* inhibits recombination in the genetic region of Chr 15 between the proximal marker *Gpt-1* and the distal marker *bt*. The pairs of crosses 7

Table 1. *Backcross linkage data for* Gpt-1 *and* Gdc-1 *with and without* Eh *in the cross. Allele symbols are given in the order* Gpt-1–Gdc-1–Eh; *a single allele symbol* a, b *or* + *indicates homozygosity for that allele*

Cross	Female × Male	Progeny genotypes				Total
		a b Eh	*ab bd+*	*a bd+*	*ab b Eh*	
1	$\frac{a\ b\ Eh}{b\ d+} \times \frac{a\ b+}{a\ b+}$	32	61	0	1	94
2	$\frac{a\ b+}{a\ b+} \times \frac{a\ b\ Eh}{b\ d+}$	27	35	0	1	63
		a b+	*ab bd+*	*a bd+*	*ab b+*	
3	$\frac{a\ b+}{b\ d+} \times \frac{a\ b+}{a\ b+}$	44	40	10	10	104
4	$\frac{a\ b+}{a\ b+} \times \frac{a\ b+}{b\ d+}$	25	32	11	5	73

Recombination estimates for *Gpt-1–Gdc-1*:

	with *Eh*	without *Eh*
*F*1 females	1/94 = 1·06±1·06	20/104 = 19·23±3·86
*F*1 males	1/63 = 1·59±1·58	16/73 = 21·92±4·84
Combined	2/157 = 1·27±0·89	36/177 = 20·34±3·03

Table 2. *Backcross linkage data for* uw, Gdc-1 *and* bt *without* Eh *present in cross. Allele symbols are given in the order* uw–Gdc-1–bt. *The* bt *locus was marked by the* bt^{2J} *allele*

Cross	Female × Male	Progeny genotypes								Total
		uw bd bt	*+b+*	*uw b+*	*+bd bt*	*uw b bt*	*+bd+*	*uw bd+*	*+b bt*	
5	$\frac{uw\ d\ bt}{+b+} \times \frac{uw\ b\ bt}{uw\ b\ bt}$	18	22	23	16	1	3	1	1	85
6	$\frac{uw\ b\ bt}{uw\ b\ bt} \times \frac{uw\ d\ bt}{+b+}$	12	4	5	5	3	0	2	0	31

Recombination estimates:

	Females	Males
uw–Gdc-1	41/85 = 48·24±5·42	13/31 = 41·94±8·86
Gdc-1–bt	6/85 = 7·06±2·78	5/51 = 16·13±6·61
uw–bt	43/85 = 50·59%	12/31 = 38·71±8·75

https://doi.org/10.1017/S0016672300035266 Published online by Cambridge University Press

Table 3. *Backcross linkage data for* uw, Gdc-1 *and* bt *with* Eh *present in cross. Allele symbols are given in the order* uw–Gdc-1–bt–Eh. *The* bt *locus was marked by the* bt^{2J} *allele*

Cross	Female × Male	Progeny genotypes								Total
		uw bd bt+	*+b+Eh*	*uw b+Eh*	*+bd bt+*	*uw bd +Eh*	*+b bt+*	*uw bd bt Eh*	*uw bd++*	
7	$\frac{uw\ d\ bt+}{+b+Eh} \times \frac{uw\ b\ bt+}{uw\ b\ bt+}$	14	28	23	24	1	1	0	2	93
8	$\frac{uw\ b\ bt+}{uw\ b\ bt+} \times \frac{uw\ d\ bt+}{+b+\ Eh}$	4	7	3	3	0	0	0	1	18
		uw d bt+	*+bd +Eh*	*uw bd +Eh*	*+d bt+*	*uw d +Eh*	*+bd bt+*	*uw d bt Eh*	*uw d++*	
9	$\frac{uw\ d\ bt+}{+b+Eh} \times \frac{uw\ d\ bt+}{uw\ d\ bt+}$	18	19	11	8	0	0	0	0	56
10	$\frac{uw\ d\ bt+}{uw\ d\ bt+} \times \frac{uw\ d\ bt+}{+b+Eh}$	46	22	33	18	0	0	0	2	121
		uw bt+	*++Eh*	*uw+Eh*	*+bt+*	*uw bt Eh*	*+++*	*uw++*	*+bt Eh*	
11	$\frac{uw\ bt+}{++Eh} \times \frac{uw\ bt+}{uw\ bt+}$	30	33	17	27	0	0	0	0	107

Recombination estimates:

	Female (cross 7)	Females (cross 9)	Females (cross 11)	Males (crosses 8 and 10)
uw–Gdc-1	47/93 = > 50%	19/56 = 33·93 ± 6·33	—	57/139 = 41·01 ± 4·17
Gdc-1–bt	4/93 = 4·30 ± 2·10	0/56 = 0%	—	3/139 = 2·16 ± 1·23
uw–bt	51/93 = > 50%	19/56 = 33·93 ± 6·33	44/107 = 41·12 ± 4·76	60/139 = 43·17 ± 4·20
uw–Eh	49/93 = > 50%	19/56 = 33·93 ± 6·33	44/107 = 41·12 ± 4·76	57/139 = 41·01 ± 4·17
Gdc-1–Eh	2/93 = 2·15 ± 1·50	0/56 = 0%	—	0/139 = 0%
bt–Eh	2/93 = 2·15 ± 1·50	0/56 = 0%	0/107 = 0%	3/139 = 2·16 ± 1·23

Table 4. *Backcross linkage data for* uw, Gpt-1 *and* Gdc-1 *without* Eh (*control crosses*). *Alleles are given in the order* uw–Gpt-1–Gdc-1

Cross	Female × Male	Progeny genotypes								Total
		uw b d	*+ab bd*	*uw ab bd*	*+b d*	*uw b bd*	*+ab d*	*uw ab d*	*+b bd*	
12	$\frac{uw\ b\ d}{+a\ b} \times \frac{uw\ b\ d}{uw\ b\ d}$	21	26	16	13	6	6	2	3	93
13	$\frac{uw\ b\ d}{uw\ b\ d} \times \frac{uw\ b\ d}{+a\ b}$	16	13	10	12	9	3	0	1	64
		uw ab bd	*+a b*	*uw a b*	*+ab bd*	*uw ab d*	*+a bd*	*uw a bd*	*+ab d*	
14	$\frac{uw\ b\ d}{+a\ b} \times \frac{uw\ a\ b}{uw\ a\ b}$	14	10	8	6	0	3	0	0	41
15	$\frac{uw\ a\ b}{uw\ a\ b} \times \frac{uw\ b\ d}{+a\ b}$	3	1	2	1	3	1	0	0	11

Recombination estimates:

	Females (crosses 12+14)	Males (crosses 13+15)
uw–Gpt-1	48/134 = 35·82 ± 4·14	25/75 = 33·33 ± 5·44
Gpt-1–Gdc-1	20/134 = 14·92 ± 3·08	17/75 = 22·67 ± 4·83
uw–Gdc-1	58/134 = 43·28 ± 4·28	41/75 = > 50%

https://doi.org/10.1017/S0016672300035266 Published online by Cambridge University Press

Table 5. *Backcross linkage data for* uw, Gpt-1 *and* Gdc-1 *with* Eh *present in cross. Alleles are given in the order* uw–Gpt-1–Gdc-1–Eh

Cross	Female × Male	Progeny genotypes								Total
		uw b d+	*+ab bd Eh*	*uw ab bd Eh*	*+b d+*	*uw b bd Eh*	*+ab d+*	*uw ab d+*	*+b bd Eh*	
16	$\frac{uw\ b\ d+}{+a\ b\ Eh} \times \frac{uw\ b\ d+}{uw\ b\ d+}$	25	27	20	19	0	3	1	1	96
17	$\frac{uw\ b\ d+}{uw\ b\ d+} \times \frac{uw\ b\ d+}{+a\ b\ Eh}$	22	36	29	17	0	0	2	0	106

Recombination estimates:

	Females	Males
uw–Gpt-1	41/96 = 42·71 ± 5·05	48/106 = 45·28 ± 4·83
Gpt-1–Gdc-1	5/96 = 5·21 ± 2·27	2/106 = 1·89 ± 1·32
uw–Gdc-1	42/96 = 43·75 ± 5·06	46/106 = 43·40 ± 4·81
uw–Eh	42/96 = 43·75 ± 5·06	46/106 = 43·40 ± 4·81
Gpt-1–Eh	5/96 = 5·21 ± 2·27	2/106 = 1·89 ± 1·32
Gdc-1–Eh	0/96 = 0%	0/106 = 0%

Table 6. *Backcross linkage data for the* Ca^{7J} *allele of the caracul locus*

Cross	Female × Male	Progeny genotypes				Total				Total
		$Ca^{7J}+$	$+Eh$	$Ca^{7J}Eh$	$++$					
18	$\frac{Ca^{7J}+}{+Eh} \times \frac{++}{++}$	46	42	0	0	88				
19	$\frac{++}{++} \times \frac{Ca^{7J}+}{+Eh}$	4	2	0	0	6				
18 and 19 combined		50	44	0	0	94				
		$uw\ bt^{2J}+$	$++Ca^{7J}$	$uw+Ca^{7J}$	$+bt^{2J}+$	$uw\ bt^{2J}$ Ca^{7J}	$+++$	$uw++$	$+bt^{2J}$ Ca^{7J}	
20	$\frac{uw\ bt^{2J}+}{++Ca^{7J}} \times \frac{uw\ bt^{2J}+}{uw\ bt^{2J}+}$	1	2	1	4	0	1	0	0	9
21	$\frac{uw\ bt^{2J}+}{uw\ bt^{2J}+} \times \frac{uw\ bt^{2J}+}{++Ca^{7J}}$	30	30	8	9	4	7	1	2	91
20 and 21 combined		31	32	9	13	4	8	1	2	100

Recombination estimates:

Ca^{7J}–*Eh*	0/94 = 0%
uw–bt^{2J}	25/100 = 25·00 ± 4·33
bt^{2J}–Ca^{7J}	15/100 = 15·00 ± 3·57
uw–Ca^{7J}	34/100 = 34·00 ± 4·74

and 9, 8 and 10, 12 and 14, and 13 and 15 are the same type of crosses involving the same loci, except that the alleles of *Gpt-1* and *Gdc-1* differed in the homozygous parent. Therefore, we show combined data for each pair of crosses except for crosses 7 and 9 in which data could not be combined because they were just barely significantly different ($P < 0{\cdot}05$). Previously unpublished linkage data for *gt* and Ca^{7J} are given in Tables 6 and 7 (crosses 18–24). No recombination was detected between either Ca^{7J} or *gt* and *Eh*, although some crossovers with *gt* could have been undetected because the cross was a partial backcross.

Recombination between *Gpt-1* and *Gdc-1* was reduced from a combined estimate in females and males of 19% to a combined estimate of 2·5% in the presence of *Eh* (Table 9; $\chi^2 = 51{\cdot}06$, D.F. = 1, $P < 0{\cdot}0001$). Although there were proportionately more *Gpt-1–Gdc-1* crossovers in cross 16, these data

https://doi.org/10.1017/S0016672300035266 Published online by Cambridge University Press

Table 7. *Backcross linkage data for* gt, Ca *and* Eh

Cross	Female × Male	Progeny genotypes				Total		Total
		gt+	+*Eh*	++	*gt Eh*			
22	$\frac{gt+}{+Eh}\times\frac{gt+}{++}$	6	21	13	0	40		
		gt Ca+	++*Eh*	+*Ca*+	*gt Ca Eh*	+*Ca Eh*	*gt*++	
23	$\frac{gt\ Ca+}{++Eh}\times\frac{gt++}{+++}$	28	59	19	0	0	0	106
24	$\frac{gt++}{+++}\times\frac{gt\ Ca+}{++Eh}$	18	81	28	0	0	0	127

Table 8. *Linkage data from outcrosses of mice doubly heterozygous for* Eh *and In18Rk to C57BL/6J mice*

Cross	Female × Male	Progeny genotypes				Total
		Eh+	+In18	*Eh* In18	++	
25	$\frac{Eh+}{+\text{In18}}\times\frac{++}{++}$	15	16	0	0	31
26	$\frac{++}{++}\times\frac{Eh+}{+\text{In18}}$	7	7	0	0	14
Crosses 25 and 26 combined		22	23	0	0	45

Table 9. *Comparison of recombination estimates among loci on Chr 15 in the presence and absence of* Eh. *These combined estimates summarize the data from Tables 1–5, crosses 1–10, 12–17. Estimates for* uw–Gdc-1 *and* uw–Eh *exclude data from crosses 7 and 9 which were significantly different from each other* ($P < 0.05$). *Estimates were combined by weighting them by the reciprocal of their variances* (*Mather, 1938*)

	Without *Eh*		With *Eh*	
Interval	Female	Male	Female	Male
uw–Gpt-1	35·82 ± 4·14	33·33 ± 5·44	42·71 ± 5·05	45·28 ± 4·83
Gpt-1–Gdc-1	16·60 ± 2·41	22·30 ± 3·42	1·80 ± 0·96	2·45 ± 0·74
uw–Gdc-1	45·19 ± 3·35	43·17 ± 5·06	41·20 ± 3·77	43·40 ± 4·81
uw–Eh	—	—	44·56 ± 3·57	42·23 ± 2·92
gt–Eh	—	—	0/144*	0/127*
Gpt-1–Eh	—	—	5·21 ± 2·27	1·89 ± 1·32
Gdc-1–Eh	—	—	0·99 ± 0·51	0·19 ± 0·19
Ca–Eh	—	—	0/194	0/133
In18Rk–*Eh*	—	—	0/31	0/14

* Partial backcrosses.

are not significantly different from those in crosses 1, 2 and 17 ($\chi^2 = 2.746$, D.F. = 1, $(0.10 < P < 0.20)$. Recombination between *Gdc-1* and *bt* appeared to be reduced slightly (females: crosses 5, 7 and 9; males: crosses 6, 8 and 10). It should be noted, however, that the expression of bt^{2J} was extremely variable in these crosses and classification of the *bt* locus was not reliable. Although bt^{2J} was also segregating in the crosses 12–17 using the Chr 15 linkage testing stock, we have not reported the data with bt^{2J} because of the

https://doi.org/10.1017/S0016672300035266 Published online by Cambridge University Press

extremely unreliable expression in these crosses. For example, in some matings that were intercrosses for bt^{2J}, the proportion of apparently *bt/bt* progeny recovered was greater than 50%; while in other matings known to be backcrosses for bt^{2J}, fewer than 25% of the progeny were scored as *bt/bt*. Even tabulating the data for manifesting (presumed *bt/bt*) classes only gave such bizarre recombination estimates for known intervals that we have omitted these data from the tabulations as well.

Recombination between *uw* and *Gpt-1* was unaffected by the presence of *Eh* (Table 9). In fact, the similarity in recombination frequencies between *uw* and *Gpt-1*, *Gdc-1* and *Eh* (Table 9) suggests that the distal segment of Chr 15, from *Gpt-1* to the telomere, segregates as a single unit in the presence of *Eh*.

(ii) *Anaphase bridge analysis and inversion crosses*

A testis from each of 34 males heterozygous for *Eh* was examined for first meiotic anaphase bridges. These animals were from various crosses for linkage analysis and maintenance of the stock. Of 556 first meiotic anaphases observed, 28 (5·04%) showed clear bridges. In our experience (Roderick, 1971) and confirmed since that time, 3·5% of anaphase I cells of normal male mice show bridges for which the cause is unknown. Any significant value above that frequency has ultimately been confirmed cytologically as the result of a paracentric inversion. Although the bridge counts in *Eh/+* males were consistently low, the chi-square for the difference between 3·5% and 5·04% is 4·42; D.F. = 1, $P < 0{\cdot}05$. This borderline significance needs confirmation, but in itself suggests the presence of a very small inversion.

Eh/+ mice had been crossed to In18Rk homozygotes to determine the extent of In18Rk on Chr 15. Table 8 shows the recombination between *Eh* and inversion In18Rk which covers the proximal half of Chr 15. Determination of the In18Rk phenotype was by anaphase bridge analysis. In18Rk heterozygous males show an anaphase bridge frequency of $36{\cdot}6 \pm 2{\cdot}4$%, and it is usually necessary to examine only 20 anaphases to distinguish In18Rk heterozygotes from normal males. There were no recombinants among 45 outcross progeny, indicating tight linkage or an overlap of the inversion with *Eh*.

Examination of testis sections from *Eh* +/+ In18Rk F1 males in this cross gave additional evidence that *Eh* is associated with an inversion. From studies of many combinations of different inversions on homologous chromosomes, we know that males heterozygous in repulsion for two different inversions that overlap a common region generally show reduced testis size, usually accompanied by sterility. Testis size can be quickly screened by observation of the slides of sectioned testes prepared for anaphase bridge analysis. Although the size difference can be definitively determined by weighing the intact testis, this is usually not necessary. Sterility is presumed by a total lack of meiotic activity in the sections and is confirmed by breeding tests (Roderick & Hawes, in preparation). In this study, all F1 males doubly heterozygous in repulsion for *Eh* and In18Rk had testes about one half normal size, although the males were meiotically and functionally fertile. These F1 males also showed the expected anaphase bridge frequency of In18Rk heterozygotes.

(iii) *Mitotic chromosome analysis*

In the Chr 15 homologs of *Eh/+* heterozygotes, the two distal dark G-bands, 15D3 and 15F, appeared to be reversed in staining intensity in one Chr 15

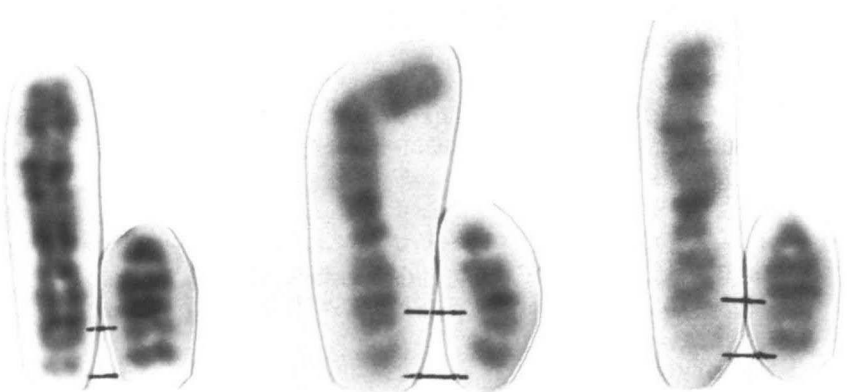

Fig. 1. Chr 15 homologs from mice heterozygous for *Eh*. The normal Chr 15, attached to Chr 3 in the Rb2Rk Robertsonian chromosome, is shown on the left and the inverted Chr 15 is on the right. The solid lines show the presumed inverted segment.

https://doi.org/10.1017/S0016672300035266 Published online by Cambridge University Press

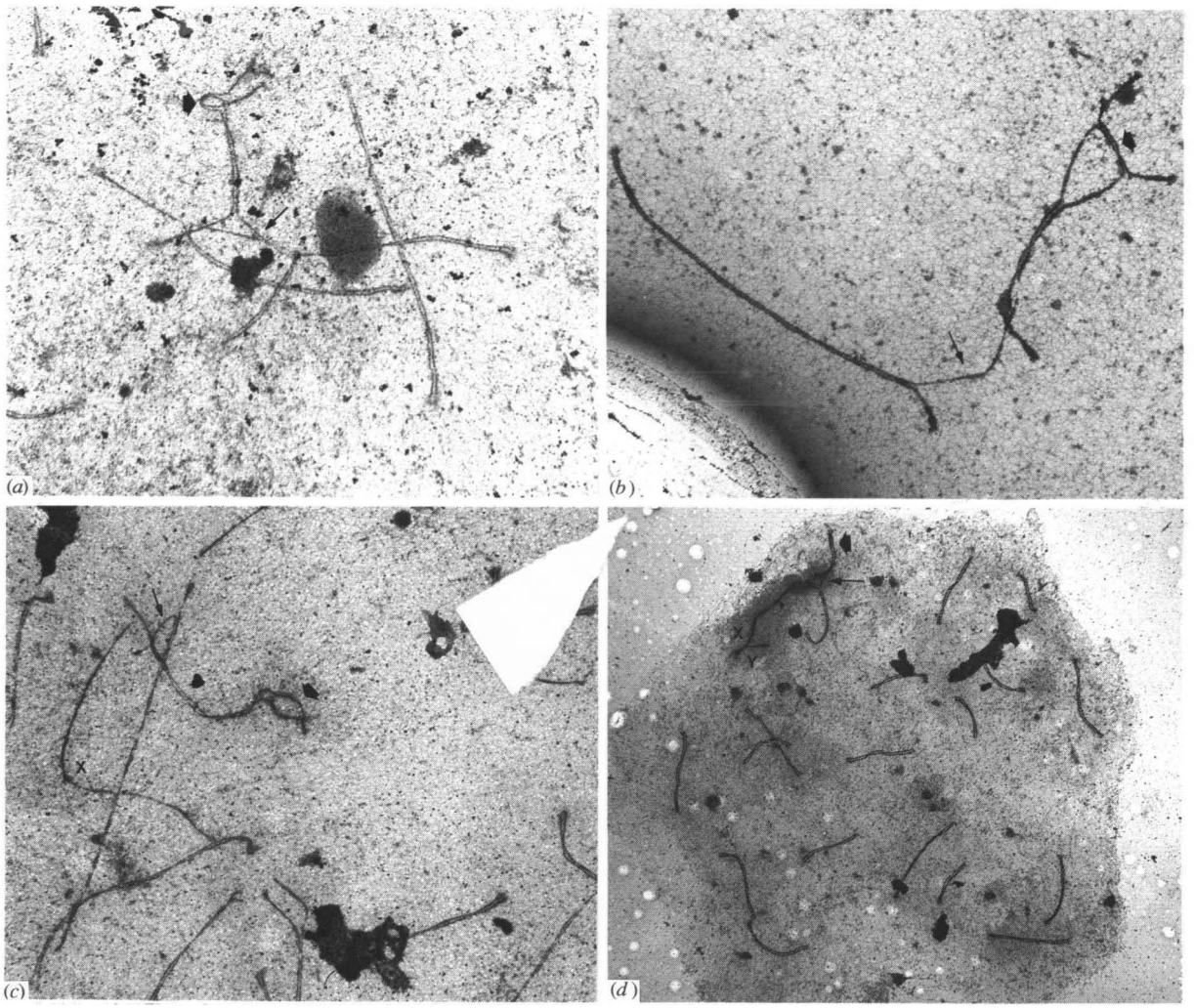

Fig. 2. Spermatocytes at pachytene showing synaptonemal complexes. The Chr 15 carrying *Eh* is the acrocentric represented by the shorter lateral element in the Robertsonian (Rb) trivalent. The delayed pairing in the centromere region of the trivalent (thin arrows) is due to heterozygosity for the Rb and not *Eh*. The different figures show (*a*) an inversion loop (broad arrow) (mag. = 6890 ×); (*b*) reverse pairing (broad arrow) (mag. = 7975 ×); (*c*) pairing failure (broad arrow) (mag. = 5425); (*d*) nonhomologous pairing so that the SC appears normally paired (mag. = 2625 ×). In (*d*) the presumed Chr 15 end of the trivalent is indicated by a broad arrow; the centromere end of Chr 15 is associated with the centromere end of the X chromosome. X and Y chromosome lateral elements are indicated by X and Y.

compared to the other. Because the difference was subtle we repeated the analysis using mice doubly heterozygous for *Eh* and a Robertsonian (Rb) chromosome, Rb(3.15)2Rk, so that the normal Chr 15 was marked by the Rb. Seventeen metaphase cells were karyotyped; additional cells were scored through the microscope. In the Chr 15 homologue involved in the Rb, the more proximal band was always darker; while in the acrocentric Chr 15 carrying the *Eh* mutation the more distal band was always darker (Fig. 1). These results again suggest a paracentric inversion extending from G-band 15D2 to the end, or near the end, of Chr 15.

To determine whether *Eh* is associated with a change in chromosomal length, total lengths of both Chr 15 homologs were measured in 17 karyotypes prepared from heterozygotes (*Eh*/+). Although the presumptive inverted segment was longer in more than half the cells, this was not corroborated by whole chromosome measurements. The results for the latter showed internal consistency within cells and between cells measured independently. A two-tailed *t*-test of the null hypothesis gave a $t = 2{\cdot}68$, D.F. = 16, $P > 0{\cdot}20$ showing no statistically significant difference in total length between the inverted and normal homologs. Thus, there is no evidence for a large deletion or duplication associated with *Eh*.

(iv) *Synaptonemal complex analysis*

In synaptonemal complex (SC) preparations the Chr 15 bivalent was marked by a Robertsonian chromosome, and the shorter chromosomal arm of the acrocentric-Robertsonian trivalent was presumed to be the Chr 15 arm. The SC preparations revealed abnormal pairing in the distal region of the Chr 15

https://doi.org/10.1017/S0016672300035266 Published online by Cambridge University Press

bivalent in a small proportion of cells. Twenty-nine per cent (7/24) of the pachytene cells scored with the light microscope exhibited either failure to pair or abnormal configurations in the distal half of Chr 15. Two of the abnormal cells appeared to have small loops and two had incomplete pairing of the lateral elements of the SC with a central region showing reverse pairing. A total of 304 cells were scored only for presence or absence of a loop configuration; the data yielded 4/304 (1·3%) cells with a loop in the Robertsonian. Examination with the electron microscope showed three classes of pairing abnormalities: (1) a small inversion-type loop in one cell (0·8%) (Fig. 2*a*), (2) an incompletely paired region with reverse pairing in the central part of the poorly paired segment in 15 cells (12·4%) (Fig. 2*b*), and (3) complete lack of pairing in the distal end of Chr 15 in 14 cells (11·6%) (Fig. 2*c*). In 10 of the 14 cells with failure to pair, the lateral element of the Chr 15 acrocentric was not paired at all with that of the Rb. The overall frequency of abnormal pairing in the cells analyzed by electron microscopy (30/121 = 24·8%) was similar to that seen at the light microscope level. An additional cell with a loop configuration and five additional cells with reverse pairing were noted in preliminary screening with the electron microscope. Most of the abnormalities were in early pachytene cells. In the remaining cells at all stages of pachytene the lateral elements of the Chr 15 bivalent appeared normally paired, suggesting that nonhomologous pairing occurs frequently. Delayed pairing between the acrocentric and Robertsonian chromosomes in the region of the centromeres was often noted (Fig. 2*d*), but this pairing delay is similar to that seen in most other Robertsonian heterozygotes (Davisson & Akeson, unpublished data). The SC data are also consistent with a paracentric inversion extending over the distal half of Chr 15.

(v) *Metaphase I analysis*

The 25 metaphase I cells scored from 2 *Eh*/+ males appeared normal with 19 autosomal bivalents plus the XY bivalent. There was no evidence for a translocation involving Chr 15, although we could not rule out an exchange too small to cause interchromosomal pairing and produce a multivalent. With the other data described above, this seems unlikely.

3. Discussion

Close association between a mutation and a chromosome rearrangement can occur in two ways: (1) one of the chromosomal aberration breakpoints interrupts or deletes a gene or (2) a mutation is induced simultaneously with the chromosomal aberration. Inseparability of the mutation and chromosomal aberration suggests either that the mutation is very near a breakpoint or that one of the breakpoints of the chromosome aberration has interrupted and mutated a gene. If the mutation can be separated from the chromosomal aberration by recombination or segregation, then the two clearly arose from simultaneous but independent events. There are examples of both. Two mutations recovered in mutagenesis experiments at the Harwell Medical Research Council (MRC) unit in England, agouti-suppressor (A^s) and bare patches (*Bpa*), were subsequently shown to be associated with paracentric chromosomal inversions (Evans & Phillips, 1975, 1978). *Bpa* was induced simultaneously with In(X)1H but has since been separated from the inversion by recombination (Evans & Phillips, 1975). The mutation A^s, on the other hand, has been inseparable from the inversion In(2)2H (Evans & Phillips, 1978). In our laboratory a recurrence of the recessive mutation pygmy (*pg*) was induced by triethylene melamine (TEM) simultaneously with the induction of inversion In(10)17Rk (Roderick, 1983). Preliminary linkage studies indicate that *pg* is located at the distal breakpoint of this inversion and in all subsequent crosses, the mutation and inversion remain inseparable (Roderick & Hawes, in preparation). At least 9 other mutations have been shown to be closely associated with reciprocal translocations (see review, Davisson & Lewis, 1990).

The mutation *Eh* also appears to be tightly associated with a chromosomal aberration. In addition to the abnormal ear phenotype, *Eh* produces many characteristics that we now know are indicative of mammalian paracentric inversions: reduced recombination with at least 10 loci spanning over 30 cM on Chr 15, inverted G-band pattern, increased anaphase bridge frequency, loops and regions of reverse pairing in synaptonemal complex (SC) configurations, and reduced testis size in double heterozygotes with In18Rk.

The genetic data clearly show that recombinants between *Eh* and several genes on distal Chr 15 are not recoverable, a classic characteristic of a chromosomal inversion. In crosses reported here and in the literature, *Eh* has shown no recombinants with *Ca* in a total of 855 opportunities (crosses 18, 19, 23 and 24; Lane & Lui, 1984). Recombinants have also not been recovered with velvet (*Ve*) (0/567) (Guenet, 1980), motor end plate disease (*med*) (0/237) (Guenet, 1976), and perinatal lethality (*ple*) (0/87) (Beier *et al.* 1989), all of which map to the same chromosomal site as *Ca* (Fig. 3). The data from our study show that the presence of *Eh* also suppresses recombination between the two more proximal markers, *Gpt-1* and *Gdc-1*, another classical characteristic of an inversion. *Eh* also shows low recombination with *Gdc-1* and *bt*, both just proximal to *Ca*. Combining the data reported here and in the literature gives recombination estimates of 0·43% between *Eh* and *bt* (crosses 7–11; Russell & McFarland, 1977) and of 0·31% between *Eh* and *Gdc-1* (crosses 1, 2, 7–10, 16 and 17). It is worth noting that all the recombinants with *bt* in the

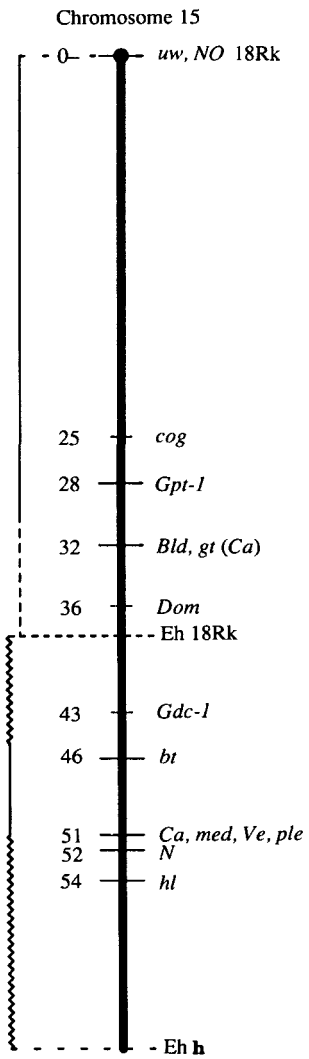

Fig. 3. Chr 15 is shown vertically with the centromere at the top and inversion In18Rk extending distally beyond dominant megacolon (*Dom*). The probable *Eh* inversion begins near or at the distal breakpoint of In18Rk and continues distally to the telomere. The solid line on the left indicating the inversion spans those loci with which an inversion does not recombine. The squiggly line indicates the probable extension of the inversion based on cytological studies of the chromosomal bands involved. Locus symbols are given to the right of the chromosome bar; the numbers to the left are approximate distances from the centromere in cm. Symbols in bold are considered anchor loci. The Chr 15 map is based on published linkage information and was generated by GBASE, a computerized genetic database for the mouse maintained by the authors at The Jackson Laboratory. The position of *Gdc-1* is based on our data and data from Hogarth *et al.* (1987); Hayakawa *et al.* (1985); Harris *et al.* (1990).

crosses reported were $+^{bt}$ $+^{Eh}$. Given the expression problems with *bt* in our crosses it is quite possible that these were not really recombinants, but were *bt* +/*bt* + mice misclassified as *bt* +/+ +. It is not stated whether the two recombinants in the 1249 mice scored by Russell & McFarland were + +/+ + or *bt Eh*/*bt* +. The *Gdc-1* phenotype and *Eh* phenotypes, however, are not likely to be misclassified, so these recombinants can not be dismissed. If the *Eh* inversion overlaps these loci, as suggested by its cytological extent, these would have to represent double crossovers. Although we would expect double crossovers to be rare in an inversion of this size, the frequency of recombination with *Gdc-1* and *bt* may be explained by the possibility that these are the only crossovers that can occur in this region of Chr 15 because of the meiotic pairing abnormalities. If *Eh* is associated with an inversion, then the SC data suggest that homologous pairing in the distal half of the Chr 15 bivalent only occurs in the center of the inversion loop (see Fig. 2*a* and 2*b*). Combined recombination estimates between *Eh* and more proximal loci are 0·45% with *cog* (Beamer *et al.* 1987), 3·5% with *Gpt-1* (crosses 1, 2, 16 and 17), 0% with *gt* (crosses 22–23) and 0·7% with *Dom* (Lane & Lui, 1984), suggesting that the effect of the presumed inversion extends as far proximal as the *cog* locus. Because the recombination estimates with *Dom* and *Gpt-1* are higher than those with *Gdc-1* and *bt*, we hypothesize that these loci are outside the inverted region.

The cytological data are also consistent with a paracentric inversion. First, the inverted G-band pattern can be most simply interpreted as a simple inversion. Second, although the first meiotic anaphase bridge frequency is only slightly higher than normal, we have never detected a significant elevation in bridge frequency that was not subsequently confirmed to be an inversion. Third, the small loops and reverse pairing seen in pachytene cells from *Eh*/+ mice clearly suggest that a segment of distal Chr 15 is reversed in orientation in the *Eh* homolog as compared to the normal homolog. Finally, the reduction in testis size in *Eh* +/+ In18Rk males is typical of that seen when two inversions that overlap the same region of the chromosome are doubly heterozygous in repulsion.

The presumptive inversion associated with *Eh*, however, behaves differently from most mammalian paracentric inversions in other characteristics. First, the anaphase bridge frequency is far below what it would normally be for an inversion of this length. This attribute is also characteristic, however, of In(4)1Dn, which was discovered cytologically rather than by elevated anaphase bridge frequency. Two other inversions, In(5)2Rk and In(15)35Rk, also have a much lower bridge frequency than their genetic lengths would suggest. In 35Rk covers more of Chr 15 than *Eh* but shares with the *Eh* inversion all the distal portion. In35Rk is also coincidentally homozygous lethal; In35Rk heterozygotes have no visible abnormal phenotype. These four inversions may differ from expectation in bridge frequency because they generally have nonhomologous or incomplete pairing in the inverted region. Either would prevent crossing over between homologous segments, a prerequisite for anaphase bridge formation.

According to Ashley (1988) one possible explanation for nonhomologous pairing is that pairing will

not proceed normally if one or both of the breakpoints is in G-dark chromatin. The Ashley hypothesis suggests that if a chromosomal rearrangement aligns G-dark and G-light chromosomal bands during synapsis, lack of homology will not be recognized and SC formation will proceed nonhomologously through the G-dark bands. In the four inversions with lower than expected anaphase bridge frequencies (described above), dark G-bands at the boundaries of the inverted regions appear to be moved intact, but it is possible that the breakpoints are at the edges of or just within the G-dark bands placing the G-dark bands near enough to the breakpoints to permit nonhomologous synapsis. The Chr 15 SC bivalent in *Eh* inversion heterozygotes shows a high frequency of nonhomologous pairing or failure to pair completely. This would reduce the opportunity for crossing over that leads to anaphase bridge. SC preparations from the other three inversions have not yet been examined in detail.

The *Eh* inversion also differs from all other inversions we have studied in that it inhibits recombination over a significant portion of the chromosome outside its limits. For the inversions with which we have done linkage studies with flanking markers, recombination is considerably enhanced over that expected between loci in the flanking regions. In the *Eh* inversion it may be that the failure to pair or nonhomologous pairing extends into the region just outside the inverted segment and reduces the opportunity for crossing over between loci in this region as well.

The genetic and meiotic and mitotic cytological data support the hypothesis that the mutation *Eh* is associated with a paracentric inversion in the distal half of Chr 15. The proposed extent of the *Eh* inversion is shown in Fig. 3. Based on our genetic and cytological data, we hypothesize that the inverted segment extends from just distal to the *Dom* locus to the distal telomere region. The suppressed genetic recombination with *cog*, *Gpt-1*, and *Dom*, loci thought to lie just outside the presumed inverted segment, can be explained by the high frequency of nonhomologous pairing or failure to pair in the involved region of Chr 15. An alternative hypothesis is that the inversion extends genetically proximal as far as the *cog* locus. Hybridization *in situ* mapping of Chr 15 by others suggests that a disproportionate amount of the present genetic map lies in the distal half of the chromosome. Data from the literature are summarized in Fig. 4. If the cytological mapping is confirmed, then all the loci indicated on the cytological map in Fig. 4 could lie within the cytological segment that is inverted in *Eh* mice (Fig. 1). If this were the case, however, the *cog*, *Gpt-1* and *Dom* loci would be just inside the inverted region and would be unlikely to cross over with *Eh*. It is likely that the *Eh* mutation is at one of the inversion breakpoints because *Eh* has not recombined with the inversion in Chr 15 in over 20 years of maintaining the stock by selecting for the *Eh* phenotype.

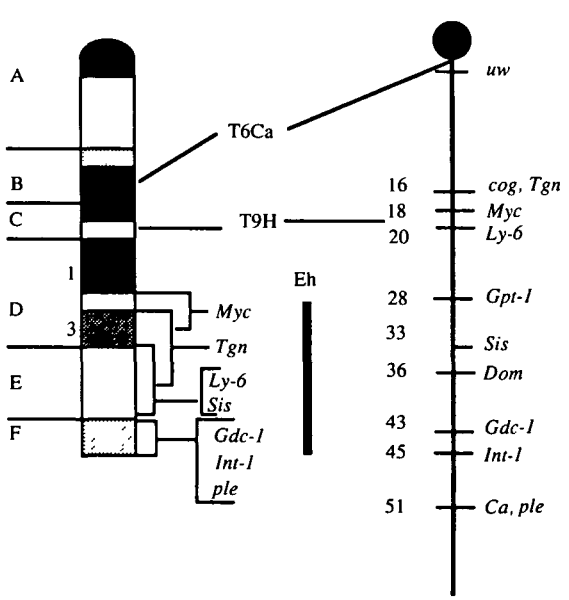

Fig. 4. A cytological diagram of Chr 15 showing C-band designations on the left and chromosomal regions to which the loci indicated have been mapped by hybridization *in situ* on the right. The data were obtained from the following sources: *Myc*, *Sis*, and *Int-1* (Adolph *et al.* 1987); *Tgn* (Hameister *et al.* 1988); *Ly-6* (LeClair *et al.* 1986); *ple* (Beier *et al.* 1989); the translocations T6Ca and T9H (Searle and Beechey, 1989). The genetic map was generated by GBASE (see Fig. 3 legend). The genetic location of *Tgn* is based on Eicher and Lee (1990). The cytological extent of the *Eh* inversion is shown as a solid vertical bar at the far right.

First and foremost, we thank Mary Lyon for innumerable helpful and thought-provoking discussions in a variety of research areas each of us has studied over the years we have known Mary. We thank Susan A. Cook, Suzanne Taylor, Nis Murphy, Cecilia Schmidt, Belinda S. Harris, Stephen H. Langley and Dr Alan L. Hillyard for technical assistance and Drs Margaret C. Green and Eva M. Eicher for helpful comments on the manuscript. The research described here was supported by National Science Foundation grant BSR 8418828, National Institutes of Health grants RR01183 and GM19656, Department of Energy Grant DE-FG02-88ER60697 and a gift from the Eleanor Naylor Dana Charitable Trust. The National Institutes of Health are not responsible for the contents of this paper nor do the comments necessarily represent official views of the NIH. The Jackson Laboratory is fully accredited by the American Association for Accreditation of Laboratory Animal Care.

References

Adolph, S., Bartram, C. R. & Hameister, H. (1987). Mapping of the oncogenes *Myc*, *Sis*, and *int-1* to the distal part of the mouse chromosome 15. *Cytogenetics Cell Genetics* **44**, 65–68.

Ashley, T. (1988). G-band position effects on meiotic synapsis and crossing over. *Genetics* **118**, 307–317.

Bangham, J. W. (1965). Hairy ears Eh. *Mouse News Letter* **33**, 68.

Bangham, J. W. (1968). Personal communication. *Mouse News Letter* **38**, 32.

Beamer, W. G., Maltais, L. J., DeBaets, M. H. & Eicher, E. M. (1987). Inherited congenital goiter in mice. *Endocrinology* **120**, 838–840.

Beier, D. R., Morton, C. C., Leder, A., Wallace, R. & Leder, P. (1989). Perinatal lethality (*ple*): a mutation caused by integration of a transgene into distal mouse chromosome 15. *Genomics* **4**, 498–504.

Davisson, M. T. & Akeson, E. C. (1987). An improved method for preparing G-banded chromosomes from mouse peripheral blood. *Cytogenetics Cell Genetics* **45**, 70–74.

Davisson, M. T. & Lewis, S. E. (1990). Chromosome aberrations associated with induced mutations effect on mapping new mutations. In press.

Dresser, M. E. & Moses, M. J. (1979). Silver staining of synaptonemal complexes in surface spreads for light and electron microscopy. *Experimental Cell Research* **121**, 416–419.

Eicher, E. M. & Lee, B. K. (1990). The NXSM recombinant inbred strains of mice: Genetic profile for 58 loci including the *Mtv* proviral loci. *Genetics* **125**, 431–446.

Eicher, E. M. & Womack, J. E. (1977). Chromosomal location of soluble glutamic-pyruvic transaminase-1 (*Gpt-1*) in the mouse. *Biochemical Genetics* **15**, 1–8.

Evans, E. P., Breckon, G. & Ford, C. E. (1964). An air-drying method for meiotic preparations from mammalian testes. *Cytogenetics* **3**, 289–294.

Evans, E. P. & Phillips, R. J. S. (1975). Inversion heterozygosity and the origin of XO daughters of *Bpa*/+ female mice. *Nature* **256**, 40.

Evans, E. P. & Phillips, R. J. S. (1978). A phenotypically marked inversion (In(2)2H). *Mouse News Letter* **58**, 44.

Guenet, J-L. (1976). Personal communication. *Mouse News Letter* **55**, 21.

Guenet, J-L. (1980). Ve and Eh. *Mouse News Letter* **62**, 72.

Hameister, H., Adolph, S., Meyer, J. & Schulz, W. A. (1988). Physical and genetic mapping around the *Myc* locus on murine chromosome 15. *Mouse News Letter* **82**, 112.

Harris, B., Akeson, E., Spencer, C., Cook, S. & Davisson, M. T. (1990). Dorsal dark stripe (dds). *Mouse News Letter* **86**, 238.

Hayakawa, J-I., Nikaido, H. & Koizumi, T. (1985). Assignment of the gene locus for the sixth component (C6) of complement in mice to chromosome 15. *Immunogenetics* **22**, 637–642.

Hogarth, P. M., McKenzie, I. F. C., Sutton, V. R., Curnow, K. M., Lee, B. N. K. & Eicher, E. M. (1987). Mapping of the mouse *Ly-6*, *Xp-14*, and *Gdc-1* loci to chromosome 15. *Immunogenetics* **25**, 21–27.

Howell, W. M. & Black, D. A. (1980). Controlled silver-staining of nucleolus organizer regions with a protective colloidal developer: a 1-step method. *Experientia* **36**, 1014–1015.

Lane, P. W. & Lui, H. M. (1984). Association of megacolon with a new dominant spotting gene (*Dom*) in the mouse. *Journal of Heredity* **75**, 435–439.

LeClair, K. P., Rabin, M., Nesbitt, M. N., Pravtcheva, D., Ruddle, F. H., Palfree, R. G. E. & Bothwell, A. (1987). Murine *Ly-6* multigene family is located on chromosome 15. *Proceedings of the National Academy of Sciences, U.S.A.* **84**, 1638–1642.

Mather, K. (1938). *Statistical Analysis in Biology*, p. 56. New York: Interscience Publishers.

Moses, M. J. (1977). Synaptonemal complex karyotyping in spermatocytes of the Chinese hamster (*Cricetulus griseus*). I. Morphology of the autosomal complement in spread preparations. *Chromosoma* **60**, 99–125.

Roderick, T. H. (1971). Producing and detecting paracentric chromosomal inversions in mice. *Mutation Research* **11**, 59–69.

Roderick, T. H. (1983). Using inversions to detect and study recessive lethals and detrimentals in mice. In *Utilization of Mammalian Specific Locus Studies in Hazard Evaluation and Estimation of Genetic Risk* (eds. F. J. de Serres and W. Sheridan), p. 135. New York: Plenum Publishing Corporation.

Russell, E. S. & McFarland, E. C. (1977). Personal communication. *Mouse News Letter* **56**, 42.

Searle, A. G. & Beechey, C. V. (1989). Map of reciprocal translocation, inversions, and insertions. In *Genetic Variants and Strains of the Laboratory Mouse* (eds. M. F. Lyon and A. G. Searle), p. 622. Oxford: Oxford University Press.

Sidman, R. L., Kinney, H. C. & Sweet, H. O. (1985). Transmissible spongiform encephalopathy in the gray tremor mutant mouse. *Proceedings of the National Academy of Sciences, U.S.A.* **82**, 253–257.